Conjugated Polymers Hot Paper

How to cite:
International Edition: doi.org/10.1002/anie.202007589
German Edition: doi.org/10.1002/ange.202007589

Ordered Solid-State Microstructures of Conjugated Polymers Arising from Solution-State Aggregation

Ze-Fan Yao, Zi-Yuan Wang, Hao-Tian Wu, Yang Lu, Qi-Yi Li, Lin Zou, Jie-Yu Wang, and Jian Pei**

Abstract: *Controlling the solution-state aggregation of conjugated polymers for producing specific microstructures remains challenging. Herein, a practical approach is developed to finely tune the solid-state microstructures through temperature-controlled solution-state aggregation and polymer crystallization. High temperature generates significant conformation fluctuation of conjugated backbones in solution, which facilitates the polymer crystallization from solvated aggregates to orderly packed structures. The polymer films deposited at high temperatures exhibit less structural disorders and higher electron mobilities (up to two orders of magnitude) in field-effect transistors, compared to those deposited at low temperatures. This work provides an effective strategy to tune the solution-state aggregation to reveal the relationship between solution-state aggregation and solid-state microstructures of conjugated polymers.*

Molecular ordering at various spatial scales of conjugated polymers in the solid state is the most critical parameter determining their charge-transport performance in functional devices, including organic solar cells, stretchable transistors, and bioelectronics.[1–6] Traditionally, researches have subscribed to the belief that the solid-state microstructures of conjugated polymers directly depend on the molecular structures.[3,7,8] However, a solution process is needed for conjugated polymers when used in the fabrication of the devices. It has been recently demonstrated that the solution-state aggregation affects solid-state microstructures and charge transport properties.[9–16] Revealing the relationship between solution-state aggregation and solid-state microstructures is a crucial aspect of organic electronics. However, conjugated polymers usually form inter-chain entanglement and complicated aggregates in solution owing to strong π–π interactions, making it difficult to probe, characterize, and control the solution-state aggregation.[17–19]

Solution-state aggregation is a general phenomenon for conjugated polymers. However, directly controlling the solution-state aggregation of conjugated polymers remains a challenge due to the lack of adequate characterization and modulation methods. Recently, considerable works have focused on the solution-state aggregation of conjugated polymers to control the solid-state microstructures and to speed up the optimization of their device performance. Efforts have been devoted to employing the effect of temperature and solvent on the polymer aggregation and microstructures. For example, Yan and co-workers demonstrated the temperature-dependent aggregation for controlling the polymer morphology.[9,10] Kim et al. reported a high-temperature solution processing to control polymer crystallization, leading to optimized microstructures and enhanced mobility.[20] Li et al. demonstrated a novel polymorphism of a diketopyrrolopyrrole (DPP) based conjugated polymer via a mixed solvent strategy, which exhibited enhanced mobility.[12] However, the effect of polymer stacking structures in solution-state aggregates and their evolutions are rarely evaluated, which critically affects the microstructures.

Herein, we report an effective approach to tune the microstructures of conjugated polymers through temperature-controlled solution-state aggregation. Multiple characterization and theoretical simulations are used to unravel the solution-state aggregation of polymers. We demonstrate that the polymer conformation, aggregate size, and thermal motion in solution can be manipulated in situ by controlling the temperature. Moreover, high temperature of polymer solutions makes it easier to overcome the energy barrier from solvated aggregates to ordered microstructures. Furthermore, polymer films deposited at higher temperatures exhibited more ordered packing and less structural disorder than the films deposited at room temperature. The orderly packed films showed much-improved carrier mobility, up to two orders of magnitudes, compared with the disordered samples.

In this work, a conjugated polymer based on four-fluorinated benzodifurandione-based oligo(*p*-phenylenevinylene) (F_4BDOPV), and 1-chloronaphthalene (CN) as solvent were adopted (Figure 1 a).[21,22] The high boiling point (260 °C) of CN provides a wide temperature window to control the polymer aggregation in solution. The solution was spin-coated onto substrates, and a liquid film was obtained due to the high boiling point of CN. Then, the liquid samples were immediately transferred onto a hotplate for solidification (Supporting Information, Figure S1). To characterize the charge transport properties of the polymer films, field-effect tran-

[*] Z.-F. Yao, Z.-Y. Wang, H.-T. Wu, Y. Lu, Q.-Y. Li, Prof. Dr. J.-Y. Wang, Prof. Dr. J. Pei
Beijing National Laboratory for Molecular Sciences (BNLMS)
Key Laboratory of Polymer Chemistry and Physics of Ministry of Education, Center of Soft Matter Science and Engineering
College of Chemistry and Molecular Engineering
Peking University, Beijing 100871 (China)
E-mail: jianpei@pku.edu.cn
Dr. L. Zou
Institute of Nuclear Physics and Chemistry
China Academy of Engineering Physics
Mianyang 621999 (China)
E-mail: jurling@pku.edu.cn
Supporting information and the ORCID identification number(s) for the author(s) of this article can be found under: https://doi.org/10.1002/anie.202007589.

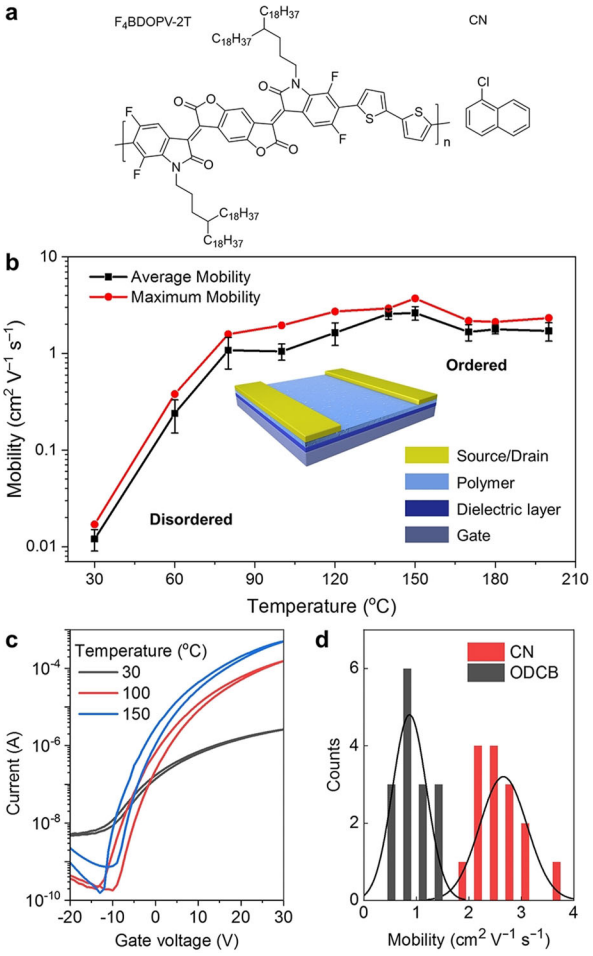

Figure 1. a) Molecular structures of F_4BDOPV-2T and 1-chloronaphthalene. b) Evolution of mobility against deposition temperature. Inset: diagram of a polymer transistor. c) Transfer characteristics of transistors with the deposition temperature of 30, 100, and 150 °C. The drain voltage is 60 V in the saturated regime, the channel width and length are 1200 and 30 μm, respectively. d) Distributions of mobilities with polymer films deposited at 150 °C using 1-chloronaphthalene (CN) and the conventional spin-coated films using *o*-dichlorobenzene (ODCB).

sistors (FETs) were fabricated. All polymer transistors exhibited reliable n-type carrier transport (Supporting Information, Figures S2–S4, and Table S1). The polymer films deposited at 30 °C exhibited the lowest electron mobility of $0.012 \pm 0.003\ cm^2 V^{-1} s^{-1}$. In contrast, when the deposition temperature was increased to 150 °C, the mobility reached $2.63 \pm 0.42\ cm^2 V^{-1} s^{-1}$, which is two orders of magnitude higher than the films deposited at 30 °C (Figure 1). The effect of contact resistance on extracted performance was excluded (Supporting Information, Figures S5, S6). Further increasing the deposition temperature resulted in a slight decrease in mobility. Significantly, the mobility of the polymer films deposited at 150 °C was enhanced to reach $2.63 \pm 0.42\ cm^2 V^{-1} s^{-1}$ with the maximum value of $3.71\ cm^2 V^{-1} s^{-1}$, which is almost three times than the mobility of films fabricated from *o*-dichlorobenzene solution of $0.87 \pm 0.31\ cm^2 V^{-1} s^{-1}$ thanks to the tuned microstructures (Figure 1 d).

These polymer films exhibited similar absorption spectra (Supporting Information, Figure S7), and similar top-surface morphology according to the atomic force microscopy images (Supporting Information, Figure S8). To gain a better illustration of the microstructures, grazing incidence wide-angle X-ray scattering (GIWAXS) experiments were conducted on these polymer films (Figure 2; Supporting Information, Figures S9–S11). Obvious out-of-plane (*h*00) diffraction peaks were recognized in all GIWAXS patterns, indicating that edge-on packing mode was adopted. As can be seen from the GIWAXS patterns, polymer films deposited at room temperature (30 °C) exhibited the weakest diffraction peaks, indicating that the polymer film was much disordered. With the deposition temperature increased to 60 °C or higher temperatures, all the diffraction peaks have become stronger, indicating that the thin film has become more ordered and crystalline. By temperature-controlled solution-state aggregation, the polymer films became more ordered than the conventional spin-coated samples using *o*-dichlorobenzene solution (Supporting Information, Figure S11). Compared to the polymer films deposited at 30 °C, the lamellar distance decreased from 29.24 to 28.55 Å with increased temperatures and retained about 28.5 Å (Figure 2 c). Meanwhile, the π–π distance in these films remained in the range of about 3.4 to 3.5 Å (Supporting Information, Table S2). Temperature-dependent lamellar distance and diffraction peak intensity demonstrate that crystallization at a higher temperature (such as 80, 140, and 150 °C) than room temperature benefits the polymer packing and results in crystalline polymer films.

To quantitatively determine the molecular ordering and crystallinity of the polymer thin films, two parameters, coherence length (L_c) and paracrystalline disorder (*g* factor), were calculated (Figure 2 c). The coherence length is commonly used to describe the size of crystalline grains in polymer thin films.[23] A larger coherence length usually indicates higher crystallinity. The paracrystalline disorder is regarded as a percentage of the mean lattice spacing, arise from the twisted backbone and packing dislocation of polymers.[24] As the deposition temperature increased from 30 to 150 °C, the polymer films exhibited increasing coherence length and decreasing paracrystalline disorder. For the polymer film deposited at 30 °C, the coherence length was only 5.97 nm (equals to 2 lamellar stacking layers), and the paracrystalline disorder was large as 19.75 %. The large paracrystalline disorder over 15 % usually represents a glass or melt, indicating high disorder in this amorphous film.[24] For the polymer film deposited at 150 °C, it showed the highest coherence length of 24.04 nm (equals to 8 lamellar stacking layers) and the lowest paracrystalline disorder of 9.72 %. Further increasing of the deposition temperature resulted in a slight decrease in the coherence length and increase in paracrystalline disorder because excessive thermal motion at higher deposition temperature can lead to more structural disorders. As consistent with the microstructure variations, higher carrier mobilities were obtained in the polymer thin films with larger grain size and less structural disorders.[25]

As conjugated polymers usually form aggregates in solution, which would significantly influent the polymer crystallization,[9,11,26] we performed in situ temperature-de-

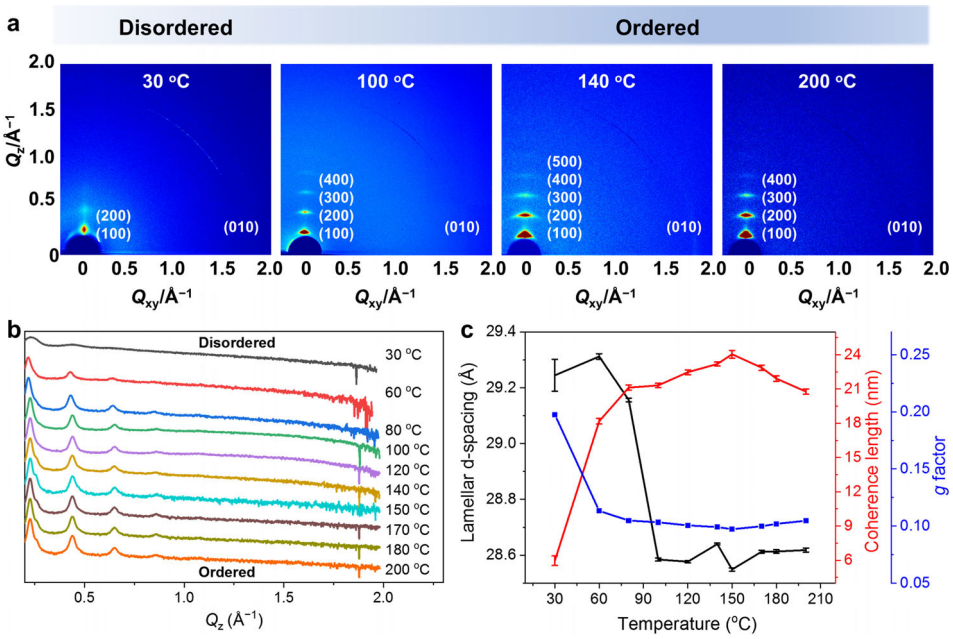

Figure 2. Molecular ordering in polymer thin films deposited at different temperatures. a) 2D GIWAXS images of polymer film deposited at 30, 100, 140, and 200 °C. b) 1D GIWAXS plots along out-of-plane direction. c) Evolution of lamellar d-spacing, coherence length, and g factor in polymer thin films deposited at different temperatures.

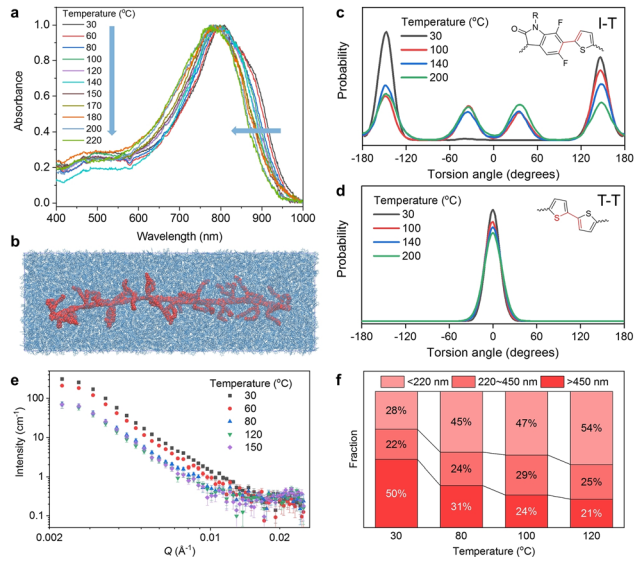

Figure 3. a) Temperature-dependent absorption spectra of F_4BDOPV-2T in 1-chloronaphthalene. b) Representative snapshot from molecular dynamics simulations of the F_4BDOPV-2T decamer in 1-chloronaphthalene. c),d) Simulated torsion angle distributions of c) isatin–thiophene (I-T) and d) thiophene–thiophene (T-T) at different temperatures. e) In situ SANS curves of the polymer solution at different temperatures. f) Size distributions of polymer aggregates at different temperatures.

pendent absorption spectroscopy, theoretical simulations, and in situ temperature-dependent small-angle neutron scattering (SANS) to obtain an in-depth understanding of the relationship between the solution-state aggregations, and solid-state microstructures. With increasing temperature from 30 to 220 °C, the absorption maximum λ_{max} at 810 nm blue-shifted to 775 nm, while another absorption peak at 884 nm almost vanished (Figure 3a). The large blueshift up to 35 nm in absorption features might result from the molecular conformation, as absorption spectra have been shown to be depended on the molecular conformation.[27,28] Thus, we confirmed that the temperature effect can induce molecular conformation variations of conjugated polymers. The conformation variations can affect the solution-state aggregation and polymer crystallization in the film-formation process,[13,29,30] which are well supported by the following experiments and simulations.

Molecular dynamics (MD) simulations are commonly used to obtain microstructures of conjugated polymers both in solution and in thin films.[31–33] We built a box contained one F_4BDOPV-2T decamer and 12000 CN molecules to simulate the polymer solution (Figure 3b; Supporting Information, Figure S12, S13). The torsion angles between conjugated units (isatin, I, and thiophene, T) were counted, as these torsion angles with single bond connections will dominate the conformation of polymer backbones.[6] We found that both torsion angles were broadened with increasing temperature (Figure 3c,d; Supporting Information, Figure S14). For the I-T dihedral angle, an evident interconversion at higher temperatures was observed, indicating more molecular conformation was induced by thermal fluctuation. For the T-T torsion, the dihedral angle conserved at all temperatures, and only slight broadening was observed. We calculated mean square displacement (MSD) of the polymer chain (Supporting Information, Figure S15). Significant MSD variation at high temperature indicates large diffusion coefficient and strong molecular motions of the polymer chain. In a word, increasing temperature leads to large thermally assisted molecular motions and increased torsion angles between conjugated units. MD results accord well with the experimental absorption spectra, as large torsion angles usually bring short effective conjugated length and blue-shift in absorption spectra. The absorption changes are supported by time-dependent density functional theory (TDDFT) calculations. With increased torsion angle between isatin and thiophene, the main absorption peak blue-shifted (Supporting Information, Figure S16). From the systematic studies, we conclude that the variation of molecular conformation of F_4BDOPV-2T can be broadened by increasing the solution temperature. Since the thermally assisted conformation trans-

formation can break the strong π–π interactions between polymer chains, controlling the temperature of polymer solution would be an effective approach to tune the polymer aggregation in solution.

To demonstrate the temperature effect on polymer aggregation in solution, in situ SANS experiments were performed.[19,34,35] The strong temperature dependence of SANS data manifested that the conjugated polymer formed large aggregates in solution owing to their strong intermolecular interactions.[36] As the temperature increased from 30 to 80 °C, the scattering intensity at the low range of the scattering vector (Q) decreased evidently, indicating the large aggregates transited to small sizes. The scattering data were fitted with the Guinier model, which gives statistical sizes of the scattering objects.[37] The apparent radius of gyration (R_g) of the polymer aggregates from the fitting data was 576, 552, 476, 473, and 456 Å at 30, 60, 80, 120, and 150 °C, respectively. The R_g decreased with the increase of the solution temperature, implying that the aggregates were broken by thermally assisted molecular motions. The size distributions of polymer aggregates in solution were also quantified using a filtration experiment (Supporting Information, Figure S17).[38,39] With increasing temperature from 30 to 120 °C, the amount of the large aggregates (diameter > 450 nm) decreased from 50 to 21 %, while the amount of the small aggregates (diameter < 220 nm) increasing from 28 to 54 % (Figure 3 f). This temperature-dependent change of the aggregate size well coincides with the SANS results.

With the above information, we proposed a possible polymer crystallization process at different temperatures (Figure 4; Supporting Information, Figure S18). At low temperatures, polymers formed large aggregates in solution, but polymer chains actually packed poorly. The weak molecular motions at low temperatures could not support the polymers to cross the high crystallization energy barrier to form orderly packed structures. Therefore, polymer chains tend to inherit the poorly packed structures from solution-state aggregates and form disordered structures (Supporting Information, Figure S18). When increasing the temperature, the high temperature will bring strong molecular motions of the polymer chains, resulting in smaller aggregates at the same time. Strong thermally assisted molecular motions will break the poorly packed structures in solution, and offer a possibility to form ordered structures.[20,30] When increasing temperature to the higher value, such as 180–200 °C in this work, the excessive thermal motions would lead to more structural disorders. Further in-depth investigation of the dynamic process during film formation will provide detailed information about polymer crystallization but is beyond the scope of this paper.[40–42] To demonstrate the generality of this strategy, two other polymers based on DPP and isoindigo building blocks were also tested, which exhibited a similar tendency of enhanced carrier mobility (Supporting Information, Figure S19). Overall, when crystallization occurred at a controlled temperature, it is easier to overcome the crystallization energy barrier. Conjugated polymers would crystallize in the way to form dense and orderly packed structures, which is propitious to charge transport.

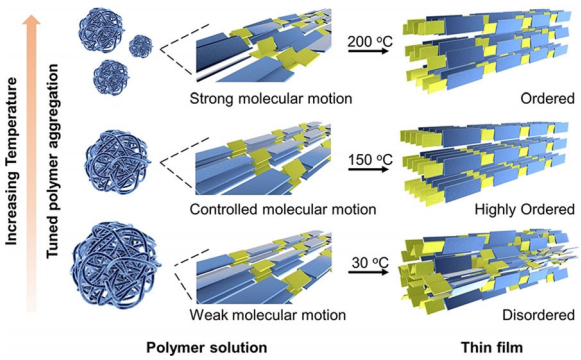

Figure 4. Diagram of the proposed polymer crystallization process from the solution-state aggregates at different temperatures.

In summary, our work develops an effective approach to tune the microstructures of conjugated polymers through the temperature-controlled solution-state aggregation. The relationship between solution-state aggregation and microstructures was fully studied. Solution temperature can critically affect polymer conformation, thermally assisted molecular motion, and aggregate size of the polymers. The strong molecular motion at high temperatures would assist the aggregated polymer to overcome the crystallization energy barrier and to form orderly packed structures. Therefore, by modulating the solution aggregation, higher crystallinity and lower lattice disorder were realized in polymer films. Field-effect transistors based on these crystalline polymer films exhibited excellent charge transport properties. Transistor devices of crystalline polymer films showed better device performance than the disordered polymer films with mobility value up to two orders of magnitude. Our work provides a simple way to tune solution-state aggregation of conjugated polymers towards high-crystallinity thin films with high device performances. We believe that our result can further advance the understanding of the relationship between solution-state aggregation and solid-state microstructures of conjugated polymers for high-performance polymer transistors, solar cells, and thermoelectrics.

Acknowledgements

This work is supported by National Key R&D Program of China (2017YFA0204701), National Natural Science Foundation of China (21420102005, 21790360, 21722201). The authors acknowledge the High-Performance Computing Platform of Peking University for supporting the computational work. The authors thank beamline BL14B1 at Shanghai Synchrotron Radiation Facility for providing the beam time.

Conflict of interest

The authors declare no conflict of interest.

Keywords: aggregation · conjugated polymers · molecular ordering · polymer transistors

[1] H. Dong, X. Fu, J. Liu, Z. Wang, W. Hu, *Adv. Mater.* **2013**, *25*, 6158 – 6183.
[2] M. Mas-Torrent, C. Rovira, *Chem. Rev.* **2011**, *111*, 4833 – 4856.
[3] D. Dang, D. Yu, E. Wang, *Adv. Mater.* **2019**, *31*, 1807019.
[4] S. Inal, J. Rivnay, A.-O. Suiu, G. G. Malliaras, I. McCulloch, *Acc. Chem. Res.* **2018**, *51*, 1368 – 1376.
[5] T. Nezakati, A. Seifalian, A. Tan, A. M. Seifalian, *Chem. Rev.* **2018**, *118*, 6766 – 6843.
[6] A. Gumyusenge, D. T. Tran, X. Luo, G. M. Pitch, Y. Zhao, K. A. Jenkins, T. J. Dunn, A. L. Ayzner, B. M. Savoie, J. Mei, *Science* **2018**, *362*, 1131 – 1134.
[7] X. Guo, A. Facchetti, T. J. Marks, *Chem. Rev.* **2014**, *114*, 8943 – 9021.
[8] J. Yang, Z. Zhao, S. Wang, Y. Guo, Y. Liu, *Chem* **2018**, *4*, 2748 – 2785.
[9] Y. Liu, J. Zhao, Z. Li, C. Mu, W. Ma, H. Hu, K. Jiang, H. Lin, H. Ade, H. Yan, *Nat. Commun.* **2014**, *5*, 5293.
[10] J. Zhao, Y. Li, G. Yang, K. Jiang, H. Lin, H. Ade, W. Ma, H. Yan, *Nat. Energy* **2016**, *1*, 15027.
[11] Y.-Q. Zheng, Z.-F. Yao, T. Lei, J.-H. Dou, C.-Y. Yang, L. Zou, X. Meng, W. Ma, J.-Y. Wang, J. Pei, *Adv. Mater.* **2017**, *29*, 1701072.
[12] M. Li, A. H. Balawi, P. J. Leenaers, L. Ning, G. H. L. Heintges, T. Marszalek, W. Pisula, M. M. Wienk, S. C. J. Meskers, Y. Yi, F. Laquai, R. A. J. Janssen, *Nat. Commun.* **2019**, *10*, 2867.
[13] K. S. Park, J. J. Kwok, R. Dilmurat, G. Qu, P. Kafle, X. Luo, S. H. Jung, Y. Olivier, J. K. Lee, J. Mei, D. Beljonne, Y. Diao, *Sci. Adv.* **2019**, *5*, eaaw7757.
[14] N.-K. Kim, S.-Y. Jang, G. Pace, M. Caironi, W.-T. Park, D. Khim, J. Kim, D.-Y. Kim, Y.-Y. Noh, *Chem. Mater.* **2015**, *27*, 8345 – 8353.
[15] Z. Wang, X. Song, Y. Jiang, J. Zhang, X. Yu, Y. Deng, Y. Han, W. Hu, Y. Geng, *Adv. Sci.* **2019**, *6*, 1902412.
[16] Y. Jiang, J. Chen, Y. Sun, Q. Li, Z. Cai, J. Li, Y. Guo, W. Hu, Y. Liu, *Adv. Mater.* **2019**, *31*, 1805761.
[17] X. Gu, L. Shaw, K. Gu, M. F. Toney, Z. Bao, *Nat. Commun.* **2018**, *9*, 534.
[18] R. Steyrleuthner, M. Schubert, I. Howard, B. Klaumünzer, K. Schilling, Z. Chen, P. Saalfrank, F. Laquai, A. Facchetti, D. Neher, *J. Am. Chem. Soc.* **2012**, *134*, 18303 – 18317.
[19] M. M. Nahid, A. Welford, E. Gann, L. Thomsen, K. P. Sharma, C. R. McNeill, *Adv. Electron. Mater.* **2018**, *4*, 1700559.
[20] Y.-J. Kim, N.-K. Kim, W.-T. Park, C. Liu, Y.-Y. Noh, D.-Y. Kim, *Adv. Funct. Mater.* **2019**, *29*, 1807786.
[21] Y.-Q. Zheng, T. Lei, J.-H. Dou, X. Xia, J.-Y. Wang, C.-J. Liu, J. Pei, *Adv. Mater.* **2016**, *28*, 7213 – 7219.
[22] Z.-F. Yao, Y.-Q. Zheng, Q.-Y. Li, T. Lei, S. Zhang, L. Zou, H.-Y. Liu, J.-H. Dou, Y. Lu, J.-Y. Wang, X. Gu, J. Pei, *Adv. Mater.* **2020**, *32*, 1806747.
[23] J. Rivnay, S. C. B. B. Mannsfeld, C. E. Miller, A. Salleo, M. F. Toney, *Chem. Rev.* **2012**, *112*, 5488 – 5519.
[24] J. Rivnay, R. Noriega, R. J. Kline, A. Salleo, M. F. Toney, *Phys. Rev. B* **2011**, *84*, 045203.
[25] Y. Olivier, D. Niedzialek, V. Lemaur, W. Pisula, K. Müllen, U. Koldemir, J. R. Reynolds, R. Lazzaroni, J. Cornil, D. Beljonne, *Adv. Mater.* **2014**, *26*, 2119 – 2136.
[26] M. M. Wienk, M. Turbiez, J. Gilot, R. A. J. Janssen, *Adv. Mater.* **2008**, *20*, 2556 – 2560.
[27] M. S. Vezie, S. Few, I. Meager, G. Pieridou, B. Dörling, R. S. Ashraf, A. R. Goñi, H. Bronstein, I. McCulloch, S. C. Hayes, M. Campoy-Quiles, J. Nelson, *Nat. Mater.* **2016**, *15*, 746 – 753.
[28] Z. Hu, R. T. Haws, Z. Fei, P. Boufflet, M. Heeney, P. J. Rossky, D. A. Vanden Bout, *Proc. Natl. Acad. Sci. USA* **2017**, *114*, 5113 – 5118.
[29] G. Qu, J. J. Kwok, Y. Diao, *Acc. Chem. Res.* **2016**, *49*, 2756 – 2764.
[30] B. Kuei, E. D. Gomez, *Soft Matter* **2017**, *13*, 49 – 67.
[31] K. Do, M. K. Ravva, T. Wang, J.-L. Brédas, *Chem. Mater.* **2017**, *29*, 346 – 354.
[32] G. Han, Y. Yi, Z. Shuai, *Adv. Energy Mater.* **2018**, *8*, 1702743.
[33] A. Ashokan, T. Wang, M. K. Ravva, J.-L. Brédas, *J. Mater. Chem. C* **2018**, *6*, 13162 – 13170.
[34] G. M. Newbloom, F. S. Kim, S. A. Jenekhe, D. C. Pozzo, *Macromolecules* **2011**, *44*, 3801 – 3809.
[35] B. McCulloch, V. Ho, M. Hoarfrost, C. Stanley, C. Do, W. T. Heller, R. A. Segalman, *Macromolecules* **2013**, *46*, 1899 – 1907.
[36] J. P. Aime, F. Bargain, M. Schott, H. Eckhardt, G. G. Miller, R. L. Elsenbaumer, *Phys. Rev. Lett.* **1989**, *62*, 55 – 58.
[37] B. Hammouda, *Polym. Rev.* **2010**, *50*, 14 – 39.
[38] H.-L. Yi, C.-C. Hua, *Macromolecules* **2019**, *52*, 332 – 340.
[39] M. Li, H. Bin, X. Jiao, M. M. Wienk, H. Yan, R. A. J. Janssen, *Angew. Chem. Int. Ed.* **2020**, *59*, 846 – 852; *Angew. Chem.* **2020**, *132*, 856 – 862.
[40] E. F. Manley, J. Strzalka, T. J. Fauvell, N. E. Jackson, M. J. Leonardi, N. D. Eastham, T. J. Marks, L. X. Chen, *Adv. Mater.* **2017**, *29*, 1703933.
[41] E. F. Manley, J. Strzalka, T. J. Fauvell, T. J. Marks, L. X. Chen, *Adv. Energy Mater.* **2018**, *8*, 1800611.
[42] X. Yi, Z. Peng, B. Xu, D. Seyitliyev, C. H. Y. Ho, E. O. Danilov, T. Kim, J. R. Reynolds, A. Amassian, K. Gundogdu, H. Ade, F. So, *Adv. Energy Mater.* **2020**, *10*, 1902430.

Manuscript received: May 27, 2020
Revised manuscript received: June 23, 2020
Accepted manuscript online: June 29, 2020
Version of record online: ■■ ■■, ■■■■

Communications

Conjugated Polymers

Z.-F. Yao, Z.-Y. Wang, H.-T. Wu, Y. Lu, Q.-Y. Li, L. Zou,* J.-Y. Wang, J. Pei* _____ ■■■■–■■■■

Ordered Solid-State Microstructures of Conjugated Polymers Arising from Solution-State Aggregation

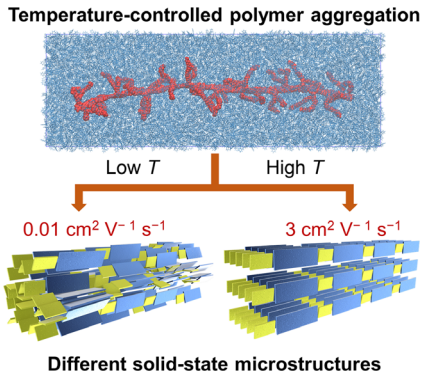

Using temperature-controlled polymer aggregation, the solid-state microstructures of conjugated polymers are finely tuned. The temperature-controlled strategy enhances the molecular ordering in thin films and leads to efficient charge transport. A polymer transistor with tuned molecular ordering exhibited improved electron mobilities of up to 3.71 $cm^2V^{-1}s^{-1}$, which is two orders of magnitude higher than the disordered samples.